A Real-Time Signal Combining System for Ka-Band Feed Arrays Using Maximum-Likelihood Weight Estimates

V. A. Vilnrotter and E. R. Rodemich
Communications Systems Research Section

A real-time digital signal combining system for use with Ka-band feed arrays is proposed. The combining system attempts to compensate for signal-to-noise ratio (SNR) loss resulting from antenna deformations induced by gravitational and atmospheric effects. The combining weights are obtained directly from the observed samples by using a "sliding-window" implementation of a vector maximum-likelihood parameter estimator. It is shown that with averaging times of about 0.1 second, combining loss for a seven-element array can be limited to about 0.1 dB in a realistic operational environment. This result suggests that the real-time combining system proposed here is capable of recovering virtually all of the signal power captured by the feed array, even in the presence of severe wind gusts and similar disturbances.

I. Introduction

There is considerable interest at the present time in operating the Deep Space Network at increasingly higher carrier frequencies for the purpose of enhancing its capabilities. To date, X-band (8.4 GHz) has been the highest carrier frequency employed for a deep-space mission due to the maturity of radio frequency (RF) components and technology at this frequency. Several recent studies concluded that Ka-band (32 GHz) is the proper next step in deep-space communications, providing 8- to 10-dB improvements in downlink telemetry capability [1]. These potential improvements can be attributed directly to the higher Ka-band carrier frequencies, which yield greater antenna gains as well as reduced sensitivity to plasma effects and increased useful bandwidth. However, there are some disadvantages associated with the use of higher carrier frequencies, namely more stringent pointing requirements, increased losses due to weather effects, and greater sensitivity to imperfections of the reflecting surfaces of the antennas [2,3]. Such imperfections become particularly troublesome on large receiving antennas, which are subject to significant gravitational and thermal deformations, focussing and collimation problems, and mechanical and wind-induced vibrations. These imperfections and pointing errors translate directly to signal loss, resulting

in a corresponding degradation in telemetry performance. However, some of the signal can be recovered by means of a properly designed feed array. Our objective is to demonstrate a compensation technique that operates with negligible combining loss and hence recovers virtually all of the signal captured by the feed array.

A conceptual design for a possible real-time antenna compensation system is shown in Fig. 1. Here it is assumed that the received signal is in the form of a temporally modulated plane wave generated by a distant spacecraft. The Cassegrain receiving system consists of a large primary reflector, a secondary reflector, a focal-plane feed array, and signal processing and combining equipment designed to reconstruct the degraded signal. A possible feed-array configuration is also shown, using a maximally compact pattern of circular feed elements. This results in a hexagonal array geometry around the central feed, with each succeeding "ring" adding six more elements than the previous ring to the total; thus, one obtains 1, 7, 19, 37, etc., array elements as the number of rings is increased.

The ideal primary reflector surface and its associated signal power distribution over the focal plane are indicated by solid curves in Fig. 1, while the deformed surface with its power distribution is shown by dashed curves. Note that antenna imperfections always increase the effective spread of the signal power in the focal plane, thus reducing the maximum possible signal power coupled into any single feed element. However, the total signal power coupled into a properly designed feed array may not be greatly reduced, although its distribution over the feeds may change with time. Therefore, it is reasonable to assume that degradations in telemetry performance can be ameliorated by the use of a matched feed array in conjuction with appropriate real-time signal processing and signal-combining techniques.

Signal-processing and combining operations should be performed in a manner compatible with proposed DSN plans and equipment for future deep-space missions; the signal-combining system must interface properly with future DSN receivers. A block diagram of the proposed DSN "Advanced Receiver" front end is shown in Fig. 2(a). This receiver was designed to operate with a single feed, thus it has only one RF input and one complex baseband output (here represented by in-phase and quadrature components). The receiver front end consists of a low-noise amplifier, a downconverter chain that generates an intermediate frequency (IF) spectrum centered around 10 MHz, an automatic gain control (AGC) circuit to maintain constant average power, an 8-bit analog-to-digital (A/D) converter operating at 40 megasamples/sec, and in-phase and quadrature phase reference samples obtained from a digital phase-locked loop, which downconverts the IF samples to baseband. The filtered outputs contain the entire modulated spectrum shifted to baseband.

As a first approximation, the front end of the proposed feed-array receiver is taken to be an array of receiver front ends (RFEs), each one associated with an element of the feed array. Under typical operating conditions, several array elements observe the signal simultaneously but with different amplitude and phase. Under favorable conditions, the distribution of signal power tends to change slowly with time as the antenna deforms due to gravitational and thermal loading. Antenna deformations and pointing errors introduced by wind gusts and turbulence-induced wavefront distortions tend to be rapidly varying effects, resulting in much less favorable conditions for reception.

A block diagram of the proposed feed-array combiner is shown in Fig. 2(b). It consists of K separate RFEs, each of which generates baseband I and Q signals that serve as inputs to a "Signal Combining System." Typically, K = 1, 7, 19, and so on. This system combines the K complex inputs and generates a single complex output. The receiver phase-locks to the residual carrier and provides an identical frequency reference to all RFEs simultaneously. Any phase difference between the reference signal and the received signal causes a measurable change in the complex output of the RFE. The signal combining system measures each complex output and uses these estimates to increase the effective signal level in the combined output.

II. NASA Telemetry Format

The telemetry format employed by deep-space vehicles has been, and presumably will continue to be, pulse code modulation/phase shift keying/phase modulation (PCM/PSK/PM) or PCM/PM [4]. In either case, the modulated carrier can be represented mathematically as [4]

$$s_T(t) = \sqrt{2P_T}\ \sin\left[\omega_c t + \sum_{i=1}^{N} \delta_i s^{(i)}(t)\right] \qquad \text{(1a)}$$

where

$$s^{(i)}(t) = \begin{cases} d_i(t) & ;\ \text{PCM/PM} \\ d_i(t)\,\mathrm{Sin}(\omega_{sci} t) & ;\ \text{PCM/PSK/PM} \end{cases} \qquad \text{(1b)}$$

δ_i is the modulation index, and $d_i(t) = \pm 1, i = 1, 2, \ldots, N$. Typically $N = 1$, although theoretically more than one data channel could be modulated simultaneously onto a carrier. For the case $N = 1$ let $\delta_i = \delta$, in which case the modulated carrier becomes

$$s_T(t) = \sqrt{2P_T}[\cos(\delta)\sin(\omega_c t) + s^{(1)}(t)\sin(\delta)\cos(\omega_c t)] \tag{2}$$

It is clear that the total received signal power is P_T watts, the power remaining in the carrier is $P_{RC} = P_T \cos^2(\delta)$ watts, and the power in the modulation sidebands is $P_M = P_T - P_{RC}$ watts. Since for $\delta = 90$ deg there is no power in the carrier component, this type of modulation is referred to as "suppressed-carrier modulation," while the term "residual-carrier modulation" is reserved for the case $0 < \delta < 90$ deg. To date, all DSN deep-space probes have employed the residual-carrier format [4]. Thus, residual-carrier modulation is assumed in this study, restricted to the case $N = 1$ for the sake of simplicity. The resulting signal spectrum consists of an impulsive term at the carrier frequency due to the residual carrier, and modulation sidebands centered around the fundamental subcarrier frequency and its harmonics.

A graphical representation of a typical received power spectrum is given in Fig. 3(a), showing spectral components around the fundamental frequency as well as around the higher-order harmonics of the square-wave subcarrier. A typical power spectrum of the complex baseband samples is shown in Fig. 3(b), consisting of a low-pass spectrum (the baseband version of the residual carrier) and the modulation spectra around the subcarrier fundamental and its harmonics. Observe that the dc component can be easily separated from the modulated subcarrier components by means of a narrow-band low-pass filter, provided the fundamental subcarrier frequency is significantly greater than the modulation bandwidth.

The effective bandwidth of this narrow low-pass filter will be denoted by B_A, whereas the effective bandwidth of the modulated subcarrier will be denoted by B_B in subsequent analysis. In particular, it will be convenient to consider digital filters that perform a finite averaging operation on the input sequence, in which case these bandwidths can be associated more precisely with the first zeros of the filter transfer function.

III. System Model

A block diagram of the signal combining system is shown in Fig. 4. The inputs to the combining system are considered to be complex samples generated by the RFEs associated with each feed. The sample bandwidth is assumed to be large compared to the subcarrier frequency so that the signal modulation is not distorted by the sampling operation. Since both the amplifier and background radiation effectively add noise to the signal, independent zero-mean complex Gaussian noise samples are added to each channel, with variance determined by the strength of the total noise process and the sample integration time. The noise-contaminated samples are split into two streams: one of these (stream A) is input to the parameter estimation subsystem, while the other (stream B) serves as input to the combining subsystem. Stream A is filtered by a bank of low-pass filters that removes the modulation sidebands in order to simplify the estimator subsystem, while stream B enters the combiner unperturbed. Thus, the samples in stream B contain both the modulation sidebands and a complex constant due to the residual carrier.

It should be emphasized that the signal-combining system considered here consists of two separate subsystems: the parameter estimator and the channel combiner. The combiner structure does not depend on the form of the parameter estimator. Thus, various types of parameter estimators could be employed to determine the required complex weights, with varying degrees of complexity and performance. Here attention shall be restricted to maximum-likelihood parameter estimators, which yield the smallest estimation errors in the absence of a priori signal and noise statistics.

The received signal in the kth channel can be modeled as

$$s_k^{(1)}(t) = \sqrt{2}S_k\left[\cos(\delta)\sin(\omega_c t + \theta_k) + s^{(1)}(t)\sin(\delta)\cos(\omega_c t + \theta_k)\right] \tag{3}$$

where θ_k and $S_k = \sqrt{P_k}$ are the unknown phase and amplitude introduced by the antenna deformation, P_k is the signal power in the kth channel, δ is the modulation index, ω_c is the carrier radian frequency (nominally $2\pi \times 32$ Grad/sec) and

$$s^{(1)}(t) = d_1(t)\,\mathrm{Sin}(\omega_{sc} t + \theta_{sc}) \tag{4}$$

is the data-modulated square-wave subcarrier at a fundamental frequency of $\omega_{sc}/2\pi$ Hz. Note that the total received signal power P_T is the sum of the individual signal powers, that is, $P_T = \sum_k P_k$. Both θ_k and S_k are assumed to be slowly varying functions of time, and may be considered constant over time intervals on the order of seconds to possibly minutes. The subcarrier phase θ_{sc} is taken to

be independent of the carrier phase θ_k, as it is typically generated by a separate oscillator on the spacecraft not coherent with the carrier.[1] Since $d(t)$ and $\mathrm{Sin}(\omega_{sc}t + \theta_{sc})$ both take on the values ± 1 at all times, it follows that $s(t)$ is also restricted to the values ± 1.

The received waveforms are downconverted to an IF frequency of about 10 MHz by means of a downconverter chain that mathematically corresponds to a single downconversion operation. It is assumed here that downconversion is performed with a "perfect" frequency reference that does not introduce any additional phase errors into the resulting IF signals. These signals can be represented as

$$\begin{aligned} s_{Ik}^{(1)}(t) &= \left[s_k^{(1)}(t)\sqrt{2}\cos\left((\omega_c - \omega_I)t\right)\right]_{LP} \\ &= S_k\left[\cos(\delta)\sin(\omega_I t + \theta_k)\right. \\ &\quad \left. + s^{(1)}(t)\sin(\delta)\cos(\omega_I t + \theta_k)\right] \end{aligned} \tag{5}$$

where "LP" refers to a low-pass filtering operation.

The IF waveforms are sampled by an A/D converter which generates 8-bit samples every T_0 seconds, or in the case of the Advanced Receiver, at a rate of 40 million samples per second. It is convenient to view these samples as the coefficients of an orthonormal expansion with basis functions the well-known "sampling functions"

$$\phi_i(t) = \frac{\sin\left[(\pi/T_0)(t - iT_0)\right]}{(\pi/T_0)(t - iT_0)} \tag{6}$$

which form a complete orthonormal set in the space of band-limited functions over the real line. In terms of these basis functions the expansion becomes

$$s_{Ik}^{(1)}(t) = \sum_{i=-\infty}^{\infty} s_{Ik}(i)\phi_i(t) \tag{7a}$$

with coefficients that represent samples of the waveform at the sampling instants "iT_0":

$$\begin{aligned} s_{Ik}(i) &= \int_{-\infty}^{\infty} s_{Ik}^{(1)}(t)\phi_i(t)dt \\ &= S_k\left[\cos(\delta)\sin(\omega_I iT_0 + \theta_k)\right. \\ &\quad \left. + s^{(1)}(iT_0)\sin(\delta)\cos(\omega_I iT_0 + \theta_k)\right] \end{aligned} \tag{7b}$$

[1] P. Kinman, Telecommunications Systems Section, personal communication.

Here it is assumed that the sampling time T_0 is small enough to avoid aliasing and that there are sufficient quantization levels to allow the representation of the quantized-amplitude samples by continuous-amplitude samples.

The final downconversion to baseband is accomplished using digital samples. Both in-phase and quadrature samples are generated simultaneously using samples of a perfect IF frequency reference, as indicated in Fig. 2(a). This operation is represented mathematically as

$${}_s s_k(i) = [2s_{Ik}(i)\sin(\omega_I iT_0)]_{LP} \tag{8a}$$

$${}_c s_k(i) = [2s_{Ik}(i)\cos(\omega_I iT_0)]_{LP} \tag{8b}$$

The sample products are filtered by digital low-pass filters that pass only the modulated subcarrier frequencies. The resulting baseband in-phase and quadrature samples in the kth channel at time iT_0 become

$${}_s s_k(i) = S_k\left[\cos(\delta)\cos(\theta_k) - s(i)\sin(\delta)\sin(\theta_k)\right] \tag{9a}$$

and

$${}_c s_k(i) = S_k\left[\cos(\delta)\sin(\theta_k) + s(i)\sin(\delta)\cos(\theta_k)\right] \tag{9b}$$

where

$$s(i) = d(iT_0)\mathrm{Sin}(\omega_{sc}iT_0 + \theta_{sc}) \tag{9c}$$

These signals contain the unknown amplitude and phase that affect both the residual-carrier and the modulated-subcarrier signals.

Making use of the identities

$$\mathrm{Re}\{e^{j\theta}[a + jb]\} = a\cos(\theta) - b\sin(\theta) \tag{10a}$$

$$\mathrm{Im}\{e^{j\theta}[a + jb]\} = a\sin(\theta) + b\cos(\theta) \tag{10b}$$

and letting $\tilde{}$ denote a complex quantity, one can also write

$${}_s s_k(i) = \mathrm{Re}\{\tilde{s}_k(i)\} \tag{11a}$$

$${}_c s_k(i) = \mathrm{Im}\{\tilde{s}_k(i)\} \tag{11b}$$

where

$$\begin{aligned} \tilde{s}_k(i) &= S_k e^{j\theta_k}\left[\cos(\delta) + js(i)\sin(\delta)\right] \\ &= \tilde{V}_k\left[\cos(\delta) + js(i)\sin(\delta)\right] \end{aligned} \tag{12}$$

is the "complex envelope" of the baseband signal samples. The complex coefficient $\tilde{V}_k$ contains both the amplitude and phase of the baseband sequences.

Next the representation of the additive noise is considered. Bandpass noise in the kth channel can be modeled as

$$n_k(t) = \sqrt{2}\left[n_{ck}(t)\cos(\omega_c t) + n_{sk}(t)\sin(\omega_c t)\right] \tag{13}$$

where $n_{ck}(t)$ and $n_{sk}(t)$ are independent zero-mean Gaussian baseband processes, each with spectral level $N_{0k}/2$.

Downconverting to IF yields

$$\begin{aligned} n_{Ik}(t) &= \left[n_k(t)\sqrt{2}\cos\{(\omega_c - \omega_I)t\}\right]_{LP} \\ &= n_{ck}(t)\cos(\omega_I t) + n_{sk}(t)\sin(\omega_I t) \end{aligned} \tag{14}$$

while the IF samples are again the coefficients of the orthonormal expansion

$$n_{Ik}(t) = \sum_{i=-\infty}^{\infty} n_{Ik}(i)\phi_i(t) \tag{15a}$$

$$\begin{aligned} n_{Ik}(i) &= \int_{-\infty}^{\infty} n_{Ik}(t)\phi_i(t)dt \\ &= n_{ck}(i)\cos(\omega_I i T_0) + n_{sk}(i)\sin(\omega_I i T_0) \end{aligned} \tag{15b}$$

Assuming that the noise processes are broadband compared to the sampling bandwidth, the correlation function of the noise samples becomes

$$\begin{aligned} E\left[n_{ck}(i)n_{ck}(\ell)\right] &= E\left[n_{sk}(i)n_{sk}(\ell)\right] \\ &= \frac{N_{0k}}{2T_0}\delta_{i\ell} \triangleq \sigma_k^2\delta_{i\ell} \end{aligned} \tag{16}$$

In-phase and quadrature noise samples are generated along with the signal samples, with the result that

$${}_s n_k(i) = \left[2n_{Ik}(i)\sin(\omega_I i T_0)\right]_{LP} = n_{sk}(i) \tag{17a}$$

and

$${}_c n_k(i) = \left[2n_{Ik}(i)\cos(\omega_I i T_0)\right]_{LP} = n_{ck}(i) \tag{17b}$$

A complex representation for the noise samples is obtained by letting

$${}_s n_k(i) = \mathrm{Re}\{\tilde{n}_k(i)\} \tag{18a}$$

$${}_c n_k(i) = \mathrm{Im}\{\tilde{n}_k(i)\} \tag{18b}$$

where

$$\tilde{n}_k(i) = n_{sk}(i) + jn_{ck}(i) \tag{18c}$$

is a sequence of complex noise samples. Note that the variance of the complex noise samples is $2\sigma_k^2$, because the real and imaginary components are independent zero-mean processes, each with variance σ_k^2. The use of complex notation will often allow considerable simplification in the derivations that follow.

Next, the problem is generalized somewhat by sampling of the primitive samples in streams A and B at different rates. The final samples are formed by averaging consecutive primitive samples, and hence represent an effective low-pass filtering operation. Since the samples in stream B must reflect the temporal variations in the modulated subcarrier accurately, typically only a few primitive samples can be averaged here. In stream A, however, enough samples must be averaged to ensure that the modulated subcarrier terms are filtered out, leaving only the residual carrier terms. Here one must be careful to make sure that the underlying processes of interest are not filtered out. Therefore, in stream A strict lower and upper bounds must be observed on the number of primitive samples averaged, while in stream B only the upper bound is relevant.

Suppose that M_A primitive samples are averaged in every channel of stream A, and M_B in stream B. This means that the time delay between samples is $T_A = M_A T_0$ in stream A and $T_B = M_B T_0$ in stream B. The situation is illustrated in Fig. 5, which shows the timing relationship between the samples in the two streams.

Applying the averaging operation of stream B to the primitive signal samples again yields Eq. (9), but evaluated at times $i_B = iM_B T_0$. The averaging operation in stream A effectively removes the subcarrier terms from the primitive samples, leaving the residual-carrier samples defined at times $i_A = iM_A T_0$:

$${}_s x_k(i_A) = \left[{}_s s_k(i)\right]_{LP} = S_k\cos(\delta)\cos(\theta_k) \tag{19a}$$

$${}_c x_k(i_A) = \left[{}_c s_k(i)\right]_{LP} = S_k\cos(\delta)\sin(\theta_k) \tag{19b}$$

Equation (19) can be expressed in complex form as

$$\begin{aligned} \tilde{x}_k(i_A) &= {}_s x_k(i_A) + j\,{}_c x_k(i_A) \\ &= S_k e^{j\theta_k}\cos(\delta) \\ &= \tilde{V}_k\cos(\delta) \triangleq \tilde{X}_k = X_{kR} + jX_{kI} \end{aligned} \tag{20}$$

Note that samples in both streams are obtained from the same sequence of primitive samples in the corresponding channels, hence the resulting sample variances in the corresponding channels are always related by the ratio of the number of primitive samples averaged in the two streams. Let the noise samples in stream A be denoted by $m_k(i_A)$, and in stream B by $n_k(i_B)$. The averaging operation reduces the noise-sample variances by factors of M_A and M_B, respectively, so that $\sigma_{Ak}^2 = \sigma_k^2/M_A$ and $\sigma_{Bk}^2 = \sigma_k^2/M_B$. The noise variances in the two streams are related by $\sigma_{Bk}^2 = \eta\sigma_{Ak}^2$, where $\eta \triangleq M_A/M_B$ is the ratio of the effective bandwidths of the two streams.

The parameter-estimation problem is greatly simplified if estimation is based only on the residual-carrier sequence as given by Eq. (20), because interference from the data modulation is not present. Since only a small fraction of the total signal power is in the residual carrier, one might expect substantial performance improvements by making use of the modulation sidebands as well. However, the more complicated estimation algorithms that make use of the full-spectrum sequence of Eq. (12) will not be addressed here. It is emphasized that while the averaging operation in stream B is optional, it is mandatory in stream A whenever modulation sidebands are present.

IV. The Combining Algorithm

The mathematical model for the combining system depicted in Fig. 4 can be summarized as follows: the noise-corrupted complex baseband samples in streams A and B are modeled as

$$\tilde{u}_k(i_A) = \tilde{x}_k(i_A) + \tilde{m}_k(i_A) \tag{21a}$$

$$\tilde{r}_k(i_B) = \tilde{s}_k(i_B) + \tilde{n}_k(i_B) \tag{21b}$$

Complex combining weights are determined by the estimator subsystem operating on stream A, and applied to the samples $\tilde{r}_k(i_B)$ in stream B to produce the combined output sequence $\tilde{z}(i_B)$:

$$\tilde{z}(i_B) = \sum_{k=1}^{K} \tilde{r}_k(i_B)\tilde{w}_k \tag{22}$$

The object of the combining algorithm is to maximize the signal-to-noise ratio of the combined output samples, defined as

$$\rho_z \triangleq \frac{|E[\tilde{z}(i_B)]|^2}{\text{var}[\tilde{z}(i_B)]} = \frac{\left|E\left[\sum_{k=1}^{K} \tilde{w}_k\tilde{r}_k(i_B)\right]\right|^2}{\text{var}\left[\sum_{k=1}^{K} \tilde{w}_k\tilde{r}_k(i_B)\right]} \tag{23}$$

Although in general ρ_z is a function of time, here it is assumed that all relevant processes are stationary, so that the time index can be ignored. Substituting Eq. (21b) for $\tilde{r}_k(i_B)$ yields

$$\rho_z = \frac{\left|\sum_{k=1}^{K} \tilde{w}_k\tilde{V}_k\left[\cos(\delta) + j\sin(\delta)s(i_B)\right]\right|^2}{\sum_{k=1}^{K} |\tilde{w}_k|^2 2\sigma_{Bk}^2} \tag{24}$$

Making use of the Schwarz inequality,

$$\left|\sum_{k=1}^{K}\left(\sqrt{2}\tilde{w}_k\sigma_{Bk}\right)\left(\frac{\tilde{V}_k}{\sqrt{2}\sigma_{Bk}}\left[\cos(\delta) + j\sin(\delta)s(i_B)\right]\right)\right|^2$$

$$\leq \sum_{k=1}^{K} |\tilde{w}_k|^2 2\sigma_{Bk}^2 \sum_{k=1}^{K} \frac{\left|\tilde{V}_k\right|^2}{2\sigma_{Bk}^2} \tag{25}$$

Dividing both sides of Eq. (25) by $\sum_k |\tilde{w}_k|^2 2\sigma_{Bk}^2$ yields the following upper bound on ρ_z:

$$\rho_z \leq \sum_{k=1}^{K} \frac{\left|\tilde{V}_k\right|^2}{2\sigma_{Bk}^2} \triangleq \rho \tag{26}$$

The choice of weights that achieves the value of the right-hand side of Eq. (26) is

$$\tilde{w}_k = \frac{\tilde{V}_k^*}{2\sigma_{Bk}^2} \tag{27a}$$

as can be seen by direct substitution

$$\rho_z = \frac{\left|\sum_{k=1}^{K} \frac{|\tilde{V}_k|^2}{2\sigma_{Bk}^2}\left[\cos(\delta) + j\sin(\delta)s(i_B)\right]\right|^2}{\sum_{k=1}^{K} \frac{|\tilde{V}_k|^2}{2\sigma_{Bk}^2}}$$

$$= \sum_{k=1}^{K} \frac{\left|\tilde{V}_k\right|^2}{2\sigma_{Bk}^2} = \rho \tag{27b}$$

Therefore, if the signal and noise parameters were known, then the combining operation defined by Eqs. (22) and (27a) would achieve the sample SNR ρ defined in Eq. (26). Note that with the optimum choice of weights, the mean value of the combined signal and the variance of the combined noise are both exactly equal to ρ. If all noise variances are equal, $\sigma_{Bk}^2 = \sigma_B^2$, then we have the interpretation $\rho = P_T/2\sigma_B^2$, where $P_T = \sum_k S_K^2$ is the total signal power collected by the array.

Since the required signal and noise parameters are generally not known, this upper bound on the sample SNR is not achieved in practice. When dealing with unknown parameters, a plausible approach is to use the best available estimates of the underlying parameters to estimate the combining weights. This is the approach adopted in this article; the estimated weights are obtained by applying the optimum weight formula (Eq. 27a) to the maximum-likelihood estimates of the underlying parameters $\{\tilde{V}_k\}$ and $\{\sigma^2_{Bk}\}$.

V. The Maximum-Likelihood Estimator

The combining algorithm requires an estimate of the complex signal coefficient $\tilde{V}_k$ and of the noise variance σ^2_{Bk}. These quantities can be estimated simultaneously from the observed samples, either in stream A or in stream B. Here attention is restricted to the residual-carrier sample stream (stream A), because of the relative simplicity of the problem when the data-modulated subcarrier is not present.

In the absence of a-priori statistics about the values of the unknown parameters $\tilde{X}_k$ and σ^2_{Bk}, the maximum-likelihood approach yields the best estimates of the embedded parameters, on the average. These estimates are obtained from the likelihood function, which is the conditional joint probability density of the observed samples, conditioned on the parameters $\tilde{X}_k$ and σ^2_{Bk}. The maximum-likelihood estimates are those values $\hat{X}_k$ and $\hat{\sigma}^2_{Bk}$ that simultaneously maximize the likelihood function, or a monotonically increasing functional of it.

The log-likelihood function is obtained from the conditional probability density of the observables, conditioned on the parameters of interest. In stream A only the residual carrier is present, hence the observed complex samples in the kth channel at time "$i_A T_A$" can be represented as

$$\tilde{u}_k(i_A) = \tilde{X}_k + \tilde{m}_k(i_A) \tag{28}$$

where $\tilde{X}_k = \tilde{V}_k \cos(\delta)$, and $\tilde{m}_k(i_A)$ is a zero-mean complex Gaussian random variable with variance $2\sigma^2_{Ak}$. It is assumed that all noise samples are independent random variables. If L consecutive samples are observed in each of K channels, the joint probability density of the entire $K \times L$ complex array becomes

$$p\left(\tilde{\mathbf{u}}|\tilde{\mathbf{X}}, \sigma^2_{\mathbf{A}}\right) = \prod_{k=1}^{K} \prod_{i_A=1}^{L} \left(2\pi\sigma^2_{Ak}\right)^{-1} e^{-|\tilde{u}_k(i_A) - \tilde{X}_k|^2 / 2\sigma^2_{Ak}} \tag{29}$$

where $\tilde{\mathbf{u}}$ is a $K \times L$-dimensional complex matrix whose elements encompass all possible values of the indices "i_A" and "k," while $\tilde{\mathbf{X}}$ and $\sigma^2_{\mathbf{A}}$ are K-dimensional complex vectors. Denoting the real and imaginary components of $\tilde{X}_k$ by X_{kR} and X_{kI}, respectively, the natural logarithm of Eq. (29) becomes

$$\begin{aligned}\Lambda &\triangleq \ln\left[p\left(\tilde{\mathbf{u}}|\tilde{\mathbf{X}}, \sigma^2_{\mathbf{A}}\right)\right] \\ &= -L\sum_{k=1}^{K} \ln(2\pi\sigma^2_{Ak}) \\ &\quad - \sum_{k=1}^{K}\left(\frac{1}{2\sigma^2_{Ak}} \sum_{i_A=1}^{L} \left[(u_{kR}(i_A) - X_{kR})^2 \right.\right. \\ &\quad \left.\left. + (u_{kI}(i_A) - X_{kI})^2\right]\right)\end{aligned} \tag{30}$$

This is called the log-likelihood function. The maximum-likelihood estimates of X_{kR}, X_{kI}, and σ^2_{Ak} are those values $\hat{X}_{kR}$, $\hat{X}_{kI}$, and $\hat{\sigma}^2_{Ak}$ that simultaneously maximize the log-likelihood function Λ. Differentiating Λ with respect to each X_{kR} and X_{kI}, setting the result equal to zero, and solving yields the maximum-likelihood estimates

$$\hat{X}_{kR} = \frac{1}{L}\sum_{i=1}^{L} u_{kR}(i_A) \tag{31a}$$

$$\hat{X}_{kI} = \frac{1}{L}\sum_{i=1}^{L} u_{kI}(i_A) \tag{31b}$$

and

$$\hat{\tilde{X}}_k = \hat{X}_{kR} + j\hat{X}_{kI} \qquad k = 1, 2, \ldots, K \tag{31c}$$

The estimate of the noise variance is obtained by writing the log-likelihood function, maximized over $\tilde{\mathbf{X}}$, as

$$\max_{\tilde{\mathbf{X}}} \Lambda = -L\sum_{k=1}^{K} \ln(2\pi\sigma^2_{Ak}) - \sum_{k=1}^{K}\left(\frac{G_k}{2\sigma^2_{Ak}}\right) \tag{32a}$$

$$G_k \triangleq \sum_{i_A=1}^{L} \left[(u_{kR}(i_A) - \hat{X}_{kR})^2 + (u_{kI}(i_A) - \hat{X}_{kI})^2\right] \tag{32b}$$

Differentiating with respect to σ^2_{Ak}, setting the result equal to zero, and solving yields

$$\hat{\sigma}^2_{Ak} = \frac{1}{2L} G_k \tag{33}$$

Note that the maximum-likelihood signal estimates $\hat{X}_{kR}$ and $\hat{X}_{kI}$ are unbiased estimates of the mean values of the real sequences $u_{kR}(i_A)$ and $u_{kI}(i_A)$, also known in statistics as the "sample mean." However, the maximum-likelihood estimates of the noise variances are biased, and hence do not correspond exactly to the unbiased "sample variance" used in statistics. Here we use the unbiased variance estimate

$$\hat{\sigma}^2_{Ak,ub} = \frac{1}{2(L-1)} G_k \tag{34}$$

For large L, the difference between the two estimates becomes negligibly small. The unbiased estimates shall be used in this analysis because each of these estimates can be modeled conveniently as the sum of the true variance plus a zero-mean error term.

The maximum-likelihood estimators defined above provide the best possible estimates of the desired parameters if a-priori statistics are not available, as long as the signal parameters and noise statistics do not change with time. These results can be extended to the slowly varying case by selecting the total observation time to be small compared to the characteristic time scale of the variations. Thus, over a short time interval the above solutions apply. However, the observation interval must now be continuously shifted in time to follow the parameter variations. This extension leads to the following "sliding-window" estimator structures:

$$\hat{\bar{X}}_k(i_A) = \frac{1}{L} \sum_{\ell=i_A-L}^{i_A-1} \tilde{u}_k(\ell) \tag{35a}$$

$$\hat{\sigma}^2_{Ak,ub}(i_A) = \frac{1}{2(L-1)} \sum_{\ell=i_A-L}^{i_A-1} \left| \tilde{u}_k(\ell) - \hat{\bar{X}}_k(i_A) \right|^2 \tag{35b}$$

Thus, the current estimates at time "$i_A T_A$" are based on the previous L samples, up to and including the sample at time "$(i_A - 1)T_A$".

For large values of L and short sample durations, the computational burden required by these estimators may become quite severe. This difficulty can be ameliorated by observing that a recursive implementation is possible, where the current estimate is obtained in terms of the previous estimate, the current observable, and the "oldest" observable in the previous sum. The recursive forms are

$$\hat{\bar{X}}_k(i_A) = \hat{\bar{X}}_k(i_A - 1) + \frac{1}{L} \left[\tilde{u}_k(i_A - 1) - \tilde{u}_k(i_A - L - 1) \right] \tag{36a}$$

$$\hat{\sigma}^2_{Ak,ub}(i_A) = \hat{\sigma}^2_{Ak,ub}(i_A - 1) + \frac{1}{2(L-1)} \Big\{ |\tilde{u}_k(i_A - 1)|^2 - |\tilde{u}_k(i_A - L - 1)|^2 - L \left[\left| \hat{\bar{X}}_k(i_A) \right|^2 - \left| \hat{\bar{X}}_k(i_A - 1) \right|^2 \right] \Big\} \tag{36b}$$

Note that the corrections to the previous estimates can be obtained from a digital "first-in, first-out" stack, minimizing the number of computations required for each update.

It is well known that the maximum-likelihood estimate of the ratio of two parameters is equivalent to the ratio of the maximum-likelihood estimates [5]. It follows that the maximum-likelihood estimate of the kth weight can be obtained from the maximum-likelihood estimates of the complex signal estimates and the noise variances as

$$\hat{w}_k(i_A) = \frac{\hat{\bar{V}}^*_k(i_A)}{2\eta\sigma^2_{Ak}(i_A)} = \frac{\hat{\bar{X}}^*_k(i_A)}{2\cos(\delta)\eta\sigma^2_{Ak}(i_A)} \tag{37}$$

The maximum-likelihood estimate of the kth weight therefore depends on the signal parameters in each channel of stream A and on the corresponding noise variances.

An interesting special case occurs if the noise variance in each channel is the same. This situation could arise if the amplifier characteristics in the various channels were exceptionally well matched and all feeds observed the same background power levels, so that the noise temperatures in the various channels were essentially the same. In this case, the common variance does not have to be estimated, since it becomes a scaling factor applied to all of the weights. Because each signal and noise term is equally scaled, the SNR of the combined noisy signal is not affected if this common scaling factor is ignored.

VI. Combiner Performance Analysis

In this section, the performance of the signal combining system will be evaluated. Constant signal components will be assumed throughout, and it shall also be assumed that L is large, so that the biased and unbiased variance estimates can be considered equal. However, the unbiased variance estimates will be used in the analysis. Performance will be evaluated in the "steady-state," that is, assuming that L or more samples have already been observed.

Assuming the "sliding-window" configuration of Eq. (35), it is seen that the estimates at time $i_A T_A$ are

based on the previous L samples, up to and including the sample at time $(i_A - 1)T_A$. Since the estimates are unbiased, each can be expressed as the sum of the true parameter plus a zero-mean random variable representing the estimation error. This model yields

$$\hat{\tilde{X}}_k(i_A) = \tilde{X}_k + \left(\hat{\tilde{X}}_k(i_A) - \tilde{X}_k\right) \triangleq \tilde{X}_k + \tilde{\epsilon}_{X_k}(i_A) \quad (38a)$$

$$\hat{\sigma}^2_{Ak}(i_A) = \sigma^2_{Ak} + (\hat{\sigma}^2_{Ak}(i_A) - \sigma^2_{Ak}) \triangleq \sigma^2_{Ak} + \epsilon_{\sigma^2_{Ak}}(i_A) \quad (38b)$$

where

$$\tilde{\epsilon}_{X_k}(i_A) = \frac{1}{L}\sum_{\ell=i_A-L}^{i_A-1}\left(\tilde{u}_k(\ell) - \tilde{X}_k\right) \quad (39a)$$

$$\epsilon_{\sigma^2_{Ak}}(i_A) = \frac{1}{2(L-1)}\sum_{\ell=i_A-L}^{i_A-1}\left|\tilde{u}_k(\ell) - \hat{\tilde{X}}_k(i_A)\right|^2 - \sigma^2_{Ak} \quad (39b)$$

Since the estimates are unbiased, it follows that the error terms are zero mean. The variance of the estimation errors can be obtained using well-known expressions for the variance of the sample mean and the variance of the sample variance, as follows:

$$\text{var}\left[\tilde{\epsilon}_{X_k}(i_A)\right] = \frac{E\left|\tilde{m}_k(i_A)\right|^2}{L} = \frac{2\sigma^2_{Ak}}{L} = \frac{2\sigma^2_{Bk}}{\eta L} \quad (40a)$$

$$\begin{aligned}\text{var}\left[\epsilon_{\sigma^2_{Ak}}(i_A)\right] &= \text{var}\left\{\frac{1}{2(L-1)}\sum_{\ell=i_A-L}^{i_A-1}\left|\tilde{u}_k(\ell) - \hat{\tilde{X}}_k(i_A)\right|^2\right\} \\ &= \frac{1}{2}\text{var}\left\{\frac{1}{(L-1)}\sum_{\ell=i_A-L}^{i_A-1}\left[u_{kR}(\ell) - \hat{X}_{kR}(i_A)\right]^2\right\} \\ &= \frac{1}{2L}\left(\mu_4 - \frac{L-3}{L-1}\sigma^4_{Ak}\right) \\ &= \frac{\sigma^4_{Ak}}{L-1} \end{aligned} \quad (40b)$$

while

$$\text{var}\left[\epsilon_{\sigma^2_{Bk}}(i_A)\right] = \frac{\eta^2\sigma^4_{Ak}}{L-1} = \frac{\sigma^4_{Bk}}{L-1} \quad (40c)$$

In deriving Eq. (40b) recall the fact that the fourth central moment of a Gaussian random variable is $\mu_4 = 3\sigma^4_{Ak}$. Since for a Gaussian population the sample mean and sample variance are independent random variables, it follows that $\tilde{\epsilon}_X(i)$ and $\epsilon_{\sigma^2_{Bk}}$ are independent as well. Since the i_Ath estimate is based on L previous samples up to and including sample number $(i_A - 1)$, and since each sample is independent of all others, it also follows that the i_Ath estimate is independent of the i_Ath sample.

Making use of the model defined in Eq. (38), the maximum-likelihood estimate of the kth weight becomes

$$\hat{\tilde{w}}_k(i_A) = \frac{\tilde{X}^*_k}{2\cos(\delta)\sigma^2_{Bk}}\left[\frac{\left(1 + \tilde{e}^*_{X_k}(i_A)\right)}{\left(1 + e_{\sigma^2_{Bk}}(i_A)\right)}\right] \quad (41a)$$

where

$$\tilde{e}^*_{X_k} = \tilde{\epsilon}^*_{X_k}/\tilde{X}^*_k \quad (41b)$$

and

$$e_{\sigma^2_{Bk}} = \epsilon_{\sigma^2_{Bk}}/\sigma^2_{Bk} \quad (41c)$$

If the standard deviation of each estimation error is small compared to the estimate, then Eq. (41a) can be approximated as

$$\begin{aligned}\hat{\tilde{w}}_k(i_A) &= \frac{\tilde{X}^*_k}{2\cos(\delta)\sigma^2_{Bk}}\left[1 + \tilde{e}^*_{X_k}(i_A)\right] \\ &\quad \times \left[1 - e_{\sigma^2_{Bk}}(i_A) + e^2_{\sigma^2_{Bk}}(i_A) - \cdots\right] \\ &\simeq \frac{\tilde{X}^*_k}{2\cos(\delta)\sigma^2_{Bk}}\left[1 + \left(\tilde{e}^*_{X_k}(i_A) - e_{\sigma^2_{Bk}}(i_A)\right)\right] \\ &\triangleq \frac{\tilde{X}^*_k}{2\cos(\delta)\sigma^2_{Bk}}\left[1 + \tilde{e}^*_{w_k}(i_A)\right] \\ &= \frac{\tilde{V}^*_k}{2\sigma^2_{Bk}}\left[1 + \tilde{e}^*_{w_k}(i_A)\right] \end{aligned} \quad (42)$$

Therefore, the weight estimates may also be expressed approximately as the sum of the true weight plus an error term, provided the errors in the component estimates are

sufficiently small. As before, the error term is zero mean, with variance

$$\begin{aligned}\text{var}\left[\tilde{e}^*_{w_k}(i_A)\right] &= \text{var}\left[\tilde{e}^*_{X_k}(i_A)\right] + \text{var}\left[e_{\sigma^2_{Bk}}(i_A)\right] \\ &= \frac{2\sigma^2_{Ak}}{\left|\tilde{X}_k\right|^2 L} + \frac{1}{(L-1)} \\ &= \frac{2\sigma^2_{Bk}}{\eta\left|\tilde{V}_k\right|^2 L\cos^2(\delta)} + \frac{1}{(L-1)} \qquad (43)\end{aligned}$$

Note that the current weight estimate is independent of the current sample, since it depends only on the previous L samples. Using the "small-error" approximation for the weighting factors, the combiner output sequence defined in Eq. (22) can be expressed as

$$\tilde{z}(i_B) \simeq \tilde{s}_c(i_B) + \tilde{n}_c(i_B) \qquad (44)$$

where

$$\tilde{s}_c(i_B) \triangleq [\cos(\delta) + j\sin(\delta)s(i_B)]\sum_{k=1}^{K}\frac{\left|\tilde{V}_k\right|^2}{2\sigma^2_{Bk}}\left[1+\tilde{e}^*_{w_k}(i_A)\right] \qquad (45a)$$

and

$$\tilde{n}_c(i_B) \triangleq \sum_{k=1}^{K}\frac{\tilde{V}^*_k\tilde{n}_k(i_B)}{2\sigma^2_{Bk}}\left[1+\tilde{e}^*_{w_k}(i_A)\right] \qquad (45b)$$

In these equations, the index i_A refers to the last estimate in stream A that occurred prior to the current sample i_B in stream B.

The combiner output in Eq. (44) can be viewed as having two components: a signal term with random magnitude that takes on a new value each time the weight index changes, plus an equivalent additive-noise term that takes on a different value for each new sample of the combined signal. The magnitude of the mean value of the signal term is ρ, the sum of the channel SNRs that would be obtained if the weights were known without error:

$$\rho = \sum_{k=1}^{K}\frac{\left|\tilde{V}_k\right|^2}{2\sigma^2_{Bk}} \qquad (46)$$

The variance of the signal term can be expressed in terms of ρ as

$$\text{var}\left[\tilde{s}_c(i_B)\right] = \frac{\rho}{\eta L\cos^2(\delta)} + \frac{1}{(L-1)}\sum_{k=1}^{K}\frac{\left|\tilde{V}_k\right|^4}{4\sigma^4_{Bk}} \qquad (47)$$

Note the dependence of the signal variance on the sum of squares of the channel SNRs in Eq. (47). This term can be bounded as follows:

$$\frac{\rho^2}{K} \le \sum_{k=1}^{K}\frac{\left|\tilde{V}_k\right|^4}{4\sigma^4_{Bk}} \le \rho^2 \qquad (48)$$

The left side follows from the Schwarz inequality: equality holds when all the channel SNRs are equal. The right side is trivial since one obtains this inequality by throwing away all of the cross terms in the square of the series for ρ. Equality holds when all the signal power is in a single channel. Useful bounds on ρ follow if the noise spectral levels in the various channels are bounded by known minimum and maximum values $N_{0\,min}$ and $N_{0\,max}$:

$$\left(\frac{P_T}{N_{0\,max}}\right)T_0M_B \triangleq \rho_l \le \rho \le \rho_u \triangleq \left(\frac{P_T}{N_{0\,min}}\right)T_0M_B \qquad (49)$$

With the help of the above bounds, the variance of the signal term can be bounded as

$$\begin{aligned}\frac{\rho_l}{\eta L\cos^2(\delta)} + \frac{\rho_l^2}{K(L-1)} &\le \text{var}\left[\tilde{s}_c(i_B)\right] \\ &\le \frac{\rho_u}{\eta L\cos^2(\delta)} + \frac{\rho_u^2}{(L-1)} \qquad (50)\end{aligned}$$

In addition to the known system parameters, these bounds involve only the total received signal power and the bounds on the noise spectral levels.

The equivalent noise term defined in Eq. (45b) consists of sums of random variables obtained from all K channels. Since the random processes in the various channels are independent, and since the current noise sample is independent of the current weight error, one can express the variance of the total complex noise as

$$\text{var}\left[\tilde{n}_c(i_B)\right] = \rho\left[1 + \frac{1}{L-1} + \frac{K}{\eta L\rho\cos^2(\delta)}\right] \qquad (51)$$

Note that the variance of the combined noise is always at least as great as the variance of the ideally weighted noise terms, ρ, approaching that limit as L grows without

bound. The excess noise terms can be attributed directly to uncertainty in the weight estimates.

Perhaps the most direct measure of combiner performance is the extent to which the sample SNR of the combined signal approaches its maximum value, ρ, which would be obtained if the complex combining weights could be determined without error. A lower value here implies degraded performance. Analogous to the previous definition in Eq. (23), the sample SNR of the combined signal when the maximum-likelihood weight estimates are used is defined as

$$\rho_{ML} = \frac{|E[\tilde{z}(i_B)]|^2}{\text{var}[\tilde{z}(i_B)]} \tag{52}$$

The time index on ρ_{ML} is ignored since all relevant processes in this model are assumed to be stationary. The magnitude of the expected value of the combiner output is again ρ, while the variance is the sum of the signal and noise variances defined in Eqs. (47) and (51):

$$\text{var}[\tilde{z}(i_B)] = \rho\left[1 + \frac{1}{L-1} + \frac{1}{\eta L\cos^2(\delta)}\left(1+\frac{K}{\rho}\right) + \frac{1}{\rho(L-1)}\sum_{k=1}^{K}\frac{\left|\tilde{V}_k\right|^4}{4\sigma_{Bk}^4}\right] \tag{53}$$

Substitution into Eq. (52) yields

$$\rho_{ML} = \frac{\rho}{\left[1 + \frac{1}{L-1} + \frac{1}{\eta L\cos^2(\delta)}\left(1+\frac{K}{\rho}\right) + \frac{1}{\rho(L-1)}\sum_{k=1}^{K}\frac{\left|\tilde{V}_k\right|^4}{4\sigma_{Bk}^4}\right]} \tag{54}$$

Note that ρ_{ML} is always less than ρ, approaching that maximum value as L approaches infinity. This is reasonable, since the maximum-likelihood weight estimates approach the true weights as the number of observed samples increases. A direct measure of the loss in sample SNR due to the imperfect weight estimates is the quantity

$$\gamma \triangleq \rho/\rho_{ML} = \gamma_s + \gamma_n \tag{55a}$$

with components due to signal, γ_s, and noise, γ_n, defined as

$$\gamma_s = \frac{1}{\eta L\cos^2(\delta)} + \frac{1}{\rho(L-1)}\sum_{k=1}^{K}\frac{\left|\tilde{V}_k\right|^4}{4\sigma_{Bk}^4} \tag{55b}$$

$$\gamma_n = 1 + \frac{1}{L-1} + \frac{K}{\eta L\rho\cos^2(\delta)} \tag{55c}$$

Since these loss factors involve both sums of the individual sample SNRs and sums of their squares, it is useful to invoke the bounds of Eqs. (48) and (49) here. Thus, the component loss factors are bounded as

$$\begin{aligned} {}_{\ell}\gamma_s &\triangleq \frac{1}{\eta L\cos^2(\delta)} + \frac{\rho_{\ell}}{K(L-1)} \le \gamma_s \\ &\le \frac{1}{\eta L\cos^2(\delta)} + \frac{\rho_u}{(L-1)} \triangleq {}_u\gamma_s \end{aligned} \tag{56a}$$

$$\begin{aligned} {}_{\ell}\gamma_n &\triangleq 1 + \frac{K}{\eta L\rho_u\cos^2(\delta)} + \frac{1}{(L-1)} \le \gamma_n \\ &\le 1 + \frac{K}{\eta L\rho_{\ell}\cos^2(\delta)} + \frac{1}{(L-1)} \triangleq {}_u\gamma_n \end{aligned} \tag{56b}$$

while the total loss is loosely bounded by sums of the upper and lower bounds on its components:

$${}_{\ell}\gamma_s + {}_{\ell}\gamma_n \triangleq {}_{\ell}\gamma \le \gamma \le {}_u\gamma \triangleq {}_u\gamma_s + {}_u\gamma_n \tag{56c}$$

Note that tighter bounds on the total combining loss exist, but these involve complicated formulas in different ranges of the parameters, and will not be considered here.

The equal noise-variance case can be treated as the general case considered above, but with considerable simplifications throughout. Although the noise variance is not estimated in this case, a common noise variance denoted by σ_B^2 shall be included in these equations for consistant results. Now the combining weights are given by

$$\hat{\tilde{w}}_k(i_A) = \frac{\hat{\tilde{X}}_k^*(i_A)}{2\cos(\delta)\sigma_B^2} \tag{57}$$

where the denominator contains σ_B^2, but not its estimate. The weight estimate can now be expressed as

$$\hat{\tilde{w}}_k(i_A) = \frac{\tilde{V}_k^*}{2\sigma_B^2}\left[1 + \tilde{\epsilon}_{X_k}^*\right] \tag{58}$$

and it is seen that there is no need to make a small-error approximation here. Therefore, these results will be valid

in general, not only where the small-error approximation holds. The variance of the combined signal and of the combined noise now becomes

$$\text{var}\,[\tilde{s}_c(i_B)] = \left(\sum_{k=1}^{K} \frac{\left|\tilde{V}_k\right|^2}{2\sigma_B^2}\right)\left(\frac{1}{\eta L \cos^2(\delta)}\right) \triangleq \frac{\rho}{\eta L \cos^2(\delta)} \tag{59a}$$

$$\text{var}\,[\tilde{n}_c(i_B)] = \rho\left[1 + \frac{K}{\eta L \rho \cos^2(\delta)}\right] \tag{59b}$$

while the variance of the total combined samples is their sum, as before:

$$\begin{aligned}\text{var}\,[\tilde{z}(i_B)] &= \text{var}\,[\tilde{s}_c(i_B)] + \text{var}\,[\tilde{n}_c(i_B)] \\ &= \rho\left[1 + \frac{\left(1 + \frac{K}{\rho}\right)}{\eta L \cos^2(\delta)}\right]\end{aligned} \tag{59c}$$

The combining loss for the equal-variance case also follows directly

$${}_e\gamma = {}_e\gamma_n + {}_e\gamma_s \tag{60a}$$

with components

$${}_e\gamma_n = 1 + \frac{K}{\eta L \rho \cos^2(\delta)} \tag{60b}$$

$${}_e\gamma_s = \frac{1}{\eta L \cos^2(\delta)} \tag{60c}$$

The behavior of the total combining loss and of its components will be examined in the next section.

VII. Numerical Results

The following example serves to illustrate the behavior of the combining loss in a realistic setting. Suppose the 70-m antenna at DSS 14 is receiving signals from a deep-space vehicle at Ka-band, and further suppose that the received power levels and noise temperatures are similar to those expected from the Galileo spacecraft during its encounter with Jupiter, that is, $P_T/N_0 = 55$ dB-Hz $= 3.16 \times 10^5$ Hz. Also assume that a standard NASA modulation format has been employed with $\delta = 80$ deg, subcarrier frequency of $f_{sc} = 2 \times 10^5$ Hz, and assume that we wish to recover the fifth subcarrier harmonic (the second and fourth harmonics are zero for a square wave) so that it is required that $f_B \geq 10^6$ Hz; let $f_B = 2 \times 10^6$ Hz. Assume a seven-element array, $K = 7$. As before, let $T_0 = 2.5 \times 10^{-8}$ sec, corresponding to a first-zero frequency of $f_0 = 1/T_0 = 4 \times 10^7$ Hz. Since the modulated subcarrier must be filtered out of stream A, the first zero of this effective filter should be at some frequency much smaller than the subcarrier fundamental, but large enough to pass the slowly-varying parameters generated by the antenna deformations. This requirement yields $f_A \leq 10^4$ Hz or so, implying that $M_A = f_0/f_A \geq 4 \times 10^3$. Observe that near the above parameter values, the "small-error" approximation upon which the general formulas are based remains valid, provided the inequality $L \gg 1$ is satisfied.

The bounds on the combining loss γ are shown in Fig. 6, for nominal P_T/N_0 of 45, 55, and 65 dB-Hz. Note that the combining-loss bounds, expressed in dB, are plotted on a logarithmic scale to show their relative behavior in regions where each combining-loss bound is very close to zero dB. The maximum and minimum values of P_T/N_0 are taken to be $\pm$ 2 dB above and below the nominal values presented in the graphs. Since the total averaging time used for each weight estimate T can be related to the number of observed samples L as $T = M_A T_0 L$, it is clear that the combining-loss bounds can be viewed either as functions of L or as functions of T. Therefore, the loss bounds are plotted in terms of both of these fundamental variables in Fig. 6. Because of the small-error approximation the bounds may not be accurate in the region $L < 10$ (or equivalently, $T < 10^{-3}$ sec), however, this region is of no interest in the present application, where the timescale of interest is typically on the order of a second. Note that a total combining loss of less than 0.1 dB can be guaranteed with observation times of less than 0.1 second, when operating at 55 dB-Hz. This result shows that during a typical encounter, this combining system can operate with negligible combining loss, even in the presence of severe wind gusts which can induce rapidly varying mechanical distortions into the antenna structure.

The components of the combining-loss bounds due to signal and noise are shown in Figs. 7(a) and 7(b), again expressed in dB, at a nominal P_T/N_0 of 65 dB-Hz, with all the other system parameters the same as above. Here the total combining-loss bounds and their components (in dB) are displayed on a linear scale in order to show the signal-loss bounds on the same graph. The loss components displayed in Fig. 7 indicate that for large L the greatest contribution to the total loss comes from the equivalent additive noise. The losses due to the random variations in the signal tend to be relatively insignificant for large L. This behavior is even more pronounced at lower P_T/N_0, where the individual components of the combining loss are even more difficult to separate. However, the reader is

cautioned that the total combining loss defined here may not be an adequate indicator of performance in all applications. The relative contribution of these loss components to the performance degradation of specific systems may differ markedly and should be carefully examined for each application.

The combining loss for the equal-variance case can be determined exactly, without resorting to small-error approximations. These results are shown in Fig. 8, which confirms the previous conclusion that total combining losses can be limited to 0.1 dB with averaging times of less than 0.1 seconds when operating at 55 dB-Hz. The behavior of the loss components shown in Fig. 9 again indicates that the dominant contribution comes from the additive noise, so that losses due to random signal variations are relatively insignificant in this region.

VIII. Summary and Conclusions

A real-time signal combining system for use with array feeds has been proposed and evaluated. The combining system can be used to compensate for losses resulting from time-varying antenna distortions due to gravitational and atmospheric effects, provided the characteristic timescale of the variations is not too rapid — perhaps on the order of a second or so. It is ideally suited for recovering losses resulting from main-reflector gravity- and wind-induced deformations of large DSN antennas operating at Ka-band or higher frequencies.

Real-time compensation is achieved by forming a weighted combination of the array-feed signals observed in the presence of additive noise with combining weights continuously adjusted to maximize the signal-to-noise ratio of the combined signal. In the digital baseband model considered, the weights were complex numbers obtained from a "maximum-likelihood" weight estimator that obtained the required signal and noise parameters from observations of the array-feed outputs. A "sliding-window" implementation was proposed that effectively follows the variations in the signal and noise parameters, achieving automatic compensation in the combined output.

A mathematical model of the real-time compensation system was developed. Performance measures were defined and system performance evaluated under a "small-error" approximation, which is valid in the regions of interest. The model assumed constant signal and noise parameters, but remains valid for time-varying parameters, provided the variations are slow compared to the time scale of the observations. It was found that the combining operation produced two distinct effects: it introduced random variations in the combined signal and it increased the effective power of the additive noise. Both of these effects could be attributed to the uncertainty in the weight estimates due to the presence of additive noise in the system. It was shown that under receiving conditions similar to those expected during the Galileo encounter, the total combining loss could be limited to 0.1 dB, with averaging times of less than a hundred milliseconds for a seven-element array. This means that virtually all of the signal power collected by the feed array can be recovered, even in the presence of wind gusts that may produce changes in the signal parameters on the timescale of a second. For larger arrays, the combining loss tends to increase.

Although two different types of degradations have been defined and quantified, their effect on telemetry symbol detection, carrier tracking loop behavior, mechanical pointing-system behavior, etc., has not been completely determined here because the interaction of these components tends to be applications-dependent. These issues should be addressed in the future. Also, mathematical models should be developed to characterize the problem in a dynamic environment and the effect of imperfect phase reference on combiner performance should be addressed. In addition, the possibility of using the entire modulated spectrum for determining the combining weights should be addressed, since this approach will improve combiner performance in the low-SNR or highly dynamic environments.

Acknowledgment

The authors would like to thank Sam Dolinar for several helpful comments and useful discussions.

References

[1] J. G. Smith, "Ka-Band (32 GHz) Downlink Capability for Deep Space Communications," *TDA Progress Report 42-88*, Jet Propulsion Laboratory, Pasadena, California, pp. 96–103, February 15, 1987.

[2] W. A. Imbriale, A. M. Bhanji, S. Blank, V. B. Lobb, R. Levy, and S. A. Rocci, "Ka-Band (32 GHz) Performance of 70-Meter Antennas in the Deep Space Network," *TDA Progress Report 42-88*, Jet Propulsion Laboratory, Pasadena, California, pp. 126–134, February 15, 1987.

[3] S. J. Blank and W. A. Imbriale, "Array Feed Synthesis for Correction of Reflector Distortion and Vernier Beam-steering," *TDA Progress Report 42-86*, Jet Propulsion Laboratory, Pasadena, California, pp. 43–55, August 15, 1986.

[4] J. H. Yuen, *Deep Space Telecommunications Systems Engineering*, Chapter 5, New York: Plenum Press, 1983.

[5] C. M. Thomas, *Maximum Likelihood Estimation of Signal-to-Noise Ratio*, Ph.D. dissertation, University of Southern California, 1967.

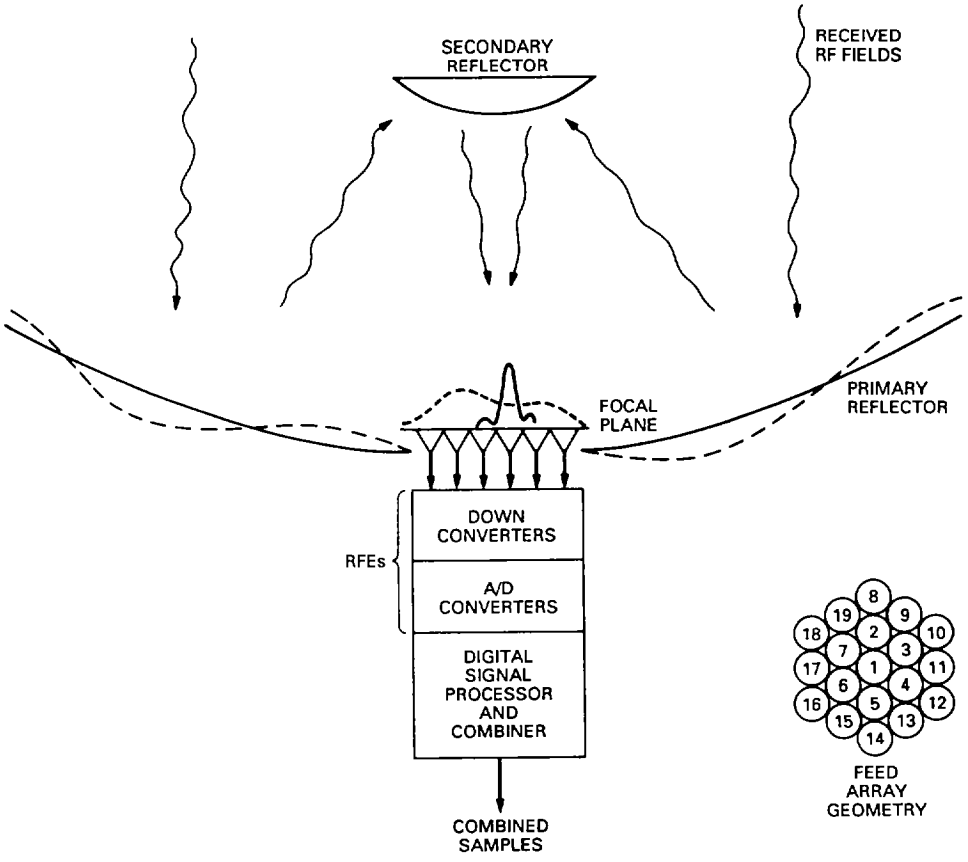

Fig. 1. Real-time antenna-compensation system conceptual design.

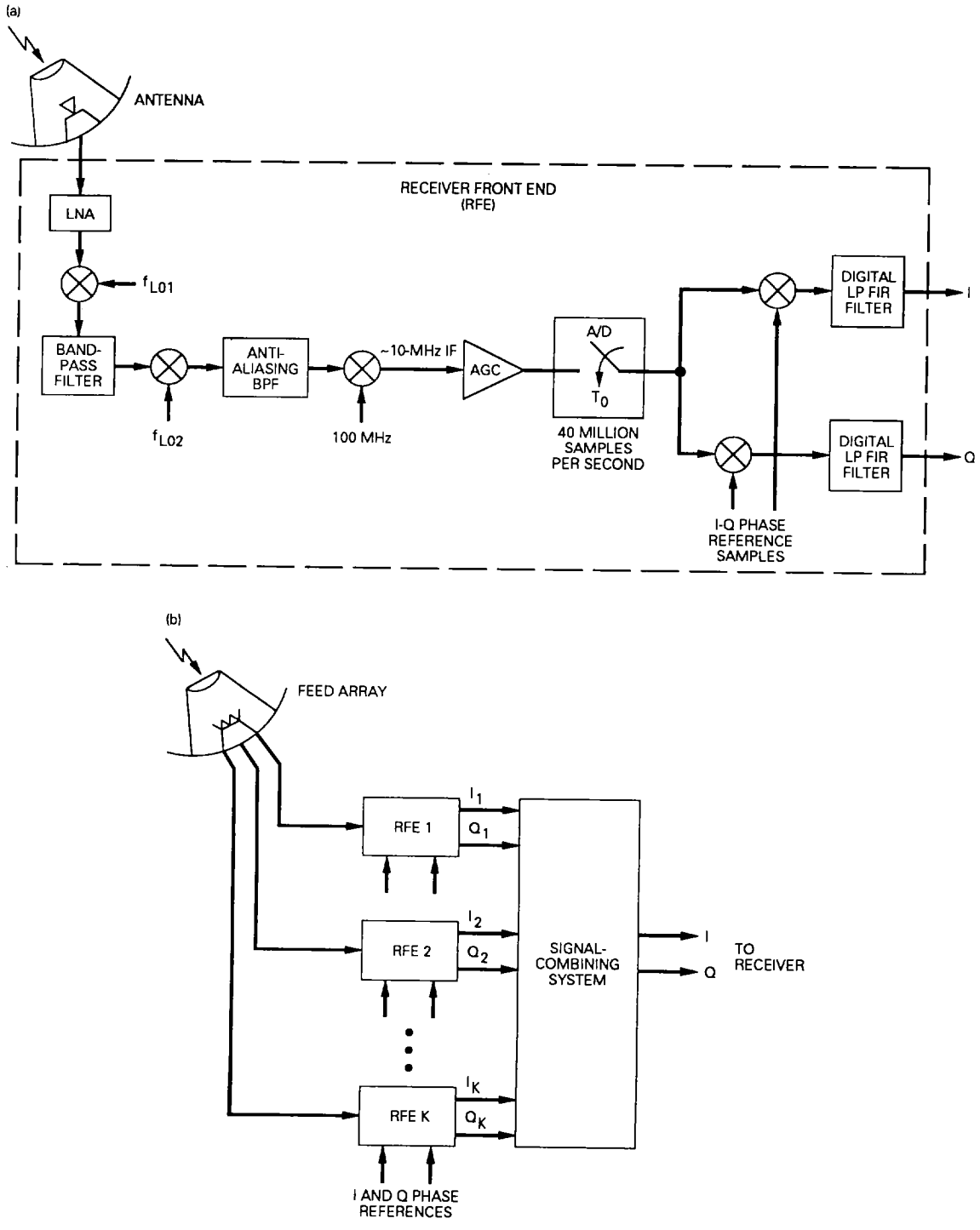

Fig. 2. System block diagrams: (a) proposed DSN Advanced Receiver front end and (b) feed-array signal-combining system.

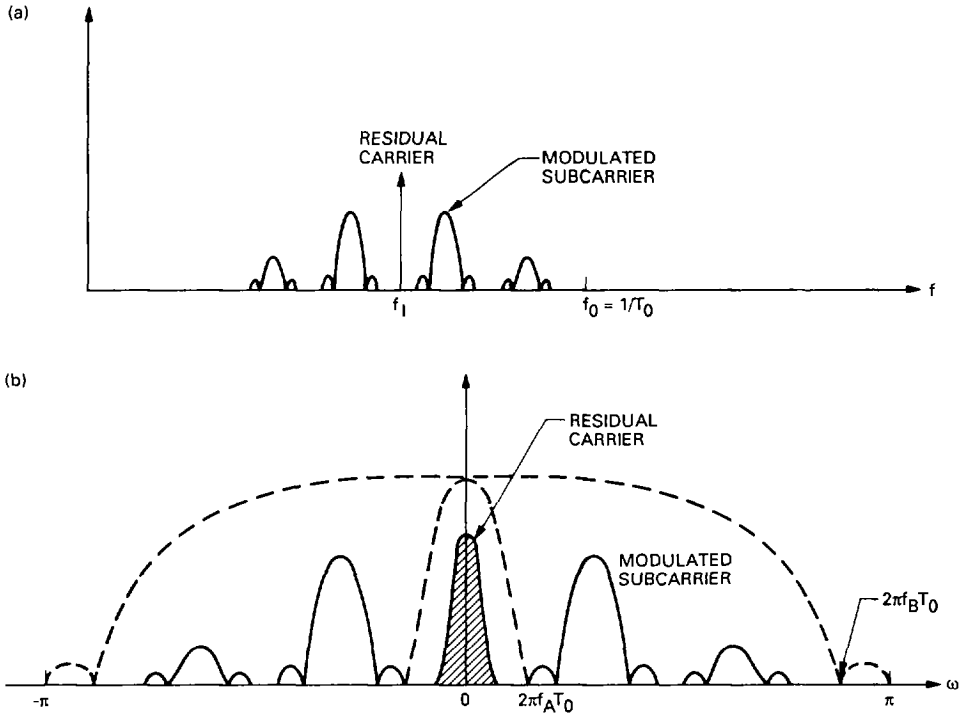

Fig. 3. NASA telemetry spectra: (a) signal spectrum after IF downconversion and (b) spectrum of baseband samples.

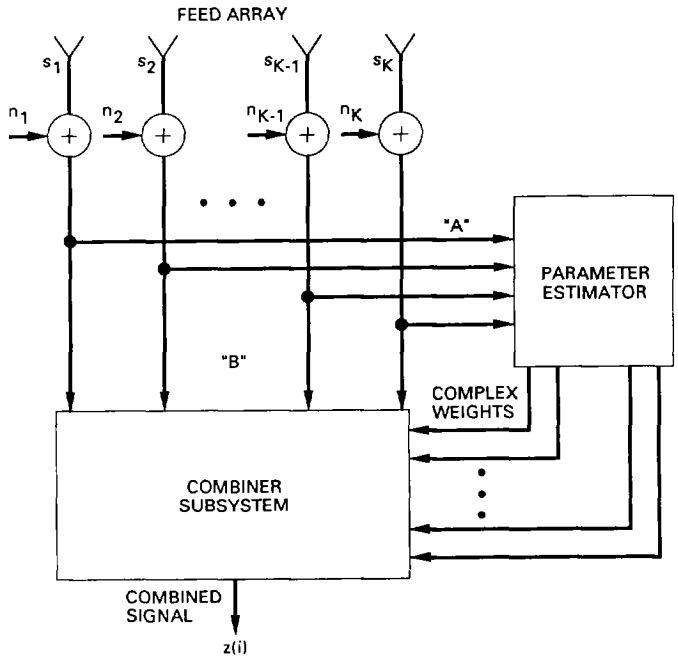

Fig. 4. Signal-combining system (baseband model) block diagram.

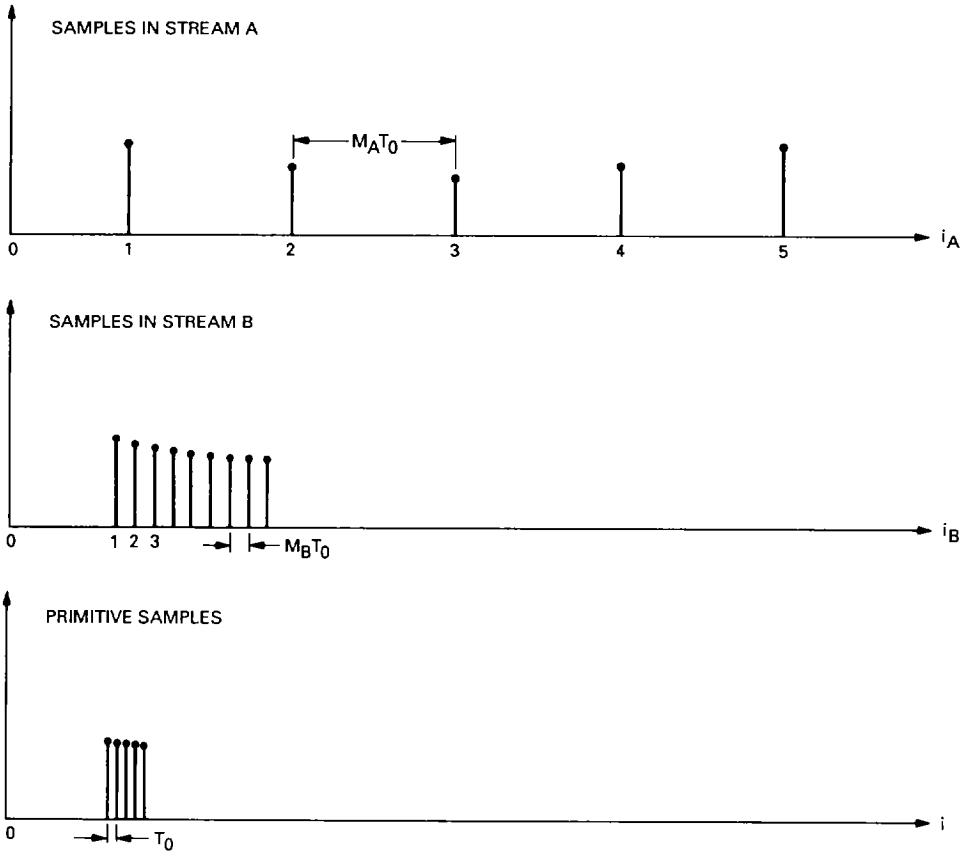

Fig. 5. Timing diagram.

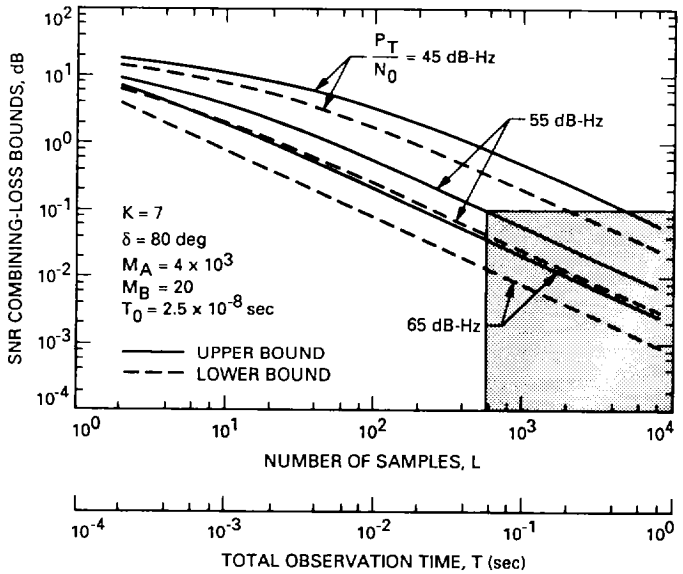

Fig. 6. SNR combining-loss bounds versus *L* and *T*.

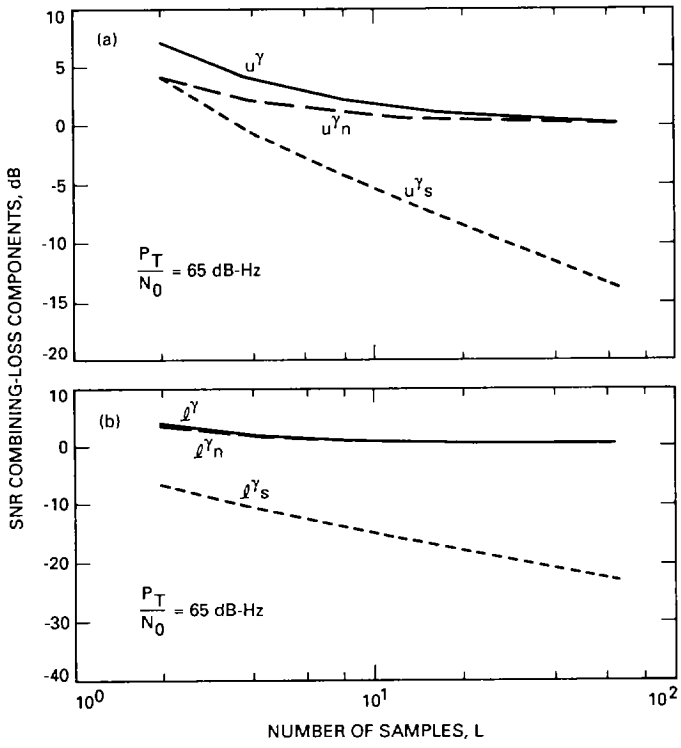

Fig. 7. SNR combining-loss components versus L (unequal-variance case): (a) upper bounds and (b) lower bounds.

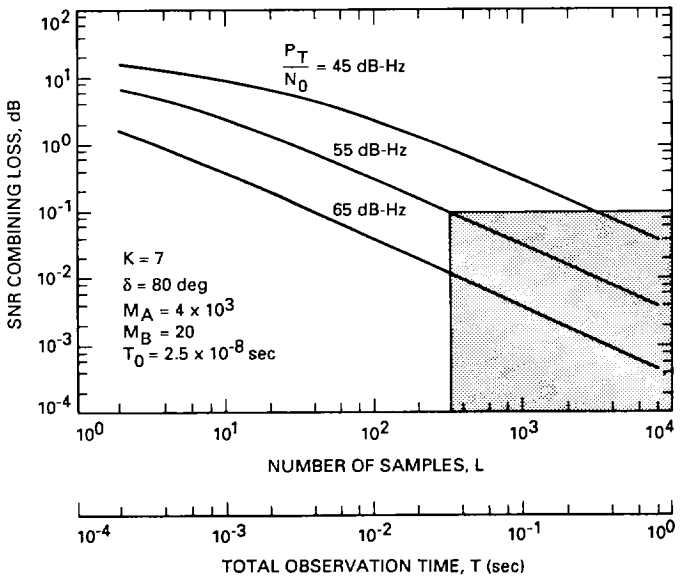

Fig. 8. SNR combining loss versus L and T (equal-variance case).

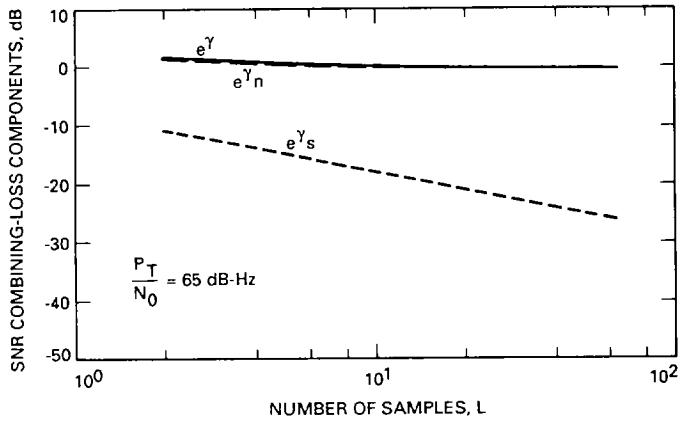

Fig. 9. SNR combining-loss components versus L (equal-variance case).